

Basic Characteristics Evaluation of a Duck-like Robot

Shuxiang Guo^{1,2,3,4*}, Zan Li^{1,2,3}, Liwei Shi^{1,2,3}, Huiming Xing^{1,2,3}, Xihuan Hou^{1,2,3},
Yu Liu^{2,3}, Huikang Liu^{2,3}, Yao Hu^{2,3}, Debin Xia^{2,3}

¹ School of Automation, Beijing Institute of Technology, No.5, Zhongguancun South Street, Haidian District, Beijing 100081, China

² Key Laboratory of Convergence Medical Engineering System and Healthcare Technology, the Ministry of Industry and Information Technology, School of Life Science, Beijing Institute of Technology, No.5, Zhongguancun South Street, Haidian District, Beijing 100081, China

³ Key Laboratory of Biomimetic Robots and Systems, Ministry of Education, Beijing Institute of Technology, No.5, Zhongguancun South Street, Haidian District, Beijing 100081, China

⁴ Faculty of Engineering, Kagawa University, 2217-20 Hayashi-cho, Takamatsu, Kagawa, Japan
E-mails: lizan@bit.edu.cn; guoshuxiang@bit.edu.cn; shiliwei@bit.edu.cn,

* Corresponding author

Abstract – Amphibious robots are the combination version of underwater and land robots. It is more versatile. Compared with simple land robot and underwater robot, it could adapt to more complex external environment, do some detective works, such as detect soil quality, detect water quality, and it could also be used for coastline patrol in military. It has a very broad development prospect. Compared with quadruped or hexapod robots, amphibious biped robots have simpler structure and easier maintenance. In this paper, a duck-like robot was developed. Firstly, this paper introduced the mechanical structure of swimming-fin of duck-like robot; secondly, introduced the hardware and software platform of the duck-like robot; thirdly, modeled and analyzed leg of this duck-like robot. Then, basic characteristics evaluation of a duck-like Robot has been carried out.

Index Terms – Duck-like Robot; Mechanical Structure of Swimming-fin; Thrust of swimming-fin;

I. INTRODUCTION

The ocean accounts for 70% of the earth surface area and has a huge amount of water resources and numerous mineral resources. In today's increasingly exhausted land resources, people turn their attention to the ocean gradually. Therefore, people are having developed a variety of robots that can be used for underwater activities to detect water bodies, or water quality detection [1].

Different underwater vehicles have different control strategies and propulsion methods. The traditional propulsion method usually takes propeller propulsion as the main propulsion mode [2]. Propeller propulsion has many advantages, such as large thrust, fast real-time response, relatively simple structure, and so on. But it also has some disadvantages, such as low propulsion efficiency, high power consumption, high noise, large volume and weight [3]. And all kinds of animals that can live in the water, such as fish, crabs, turtles and other animals, have been evolved continuously, and have a very strong swimming ability, fast swimming speed, low noise, and high propulsion efficiency [4]. Research on bionic

underwater vehicles was being carried out gradually in recent years[5].

Wang *et al.* use Computational Fluid Dynamics (CFD) to do a numerical simulation analysis on a bionic robotic fish [6]. This paper reveals the relationship between fish body shape and swimming performance, and provides references for the shape design and performance optimization of robotic fish in the future.

Wicaksono *et al.* research anatomy and biomechanics in the view of terrestrial locomotion on a tree-climbing fish [7]. They researched the relationship of pectoral fin movement with pelvic fin movement. This research could provide ideas and greater potential for the development of energetically more efficient systems of ambulation in biomimetic robot.

Wang *et al.* designed a bionic robotic fish. This fish use the powerful tail to provide the propulsion, the pectoral fins are used to regulate the direction of the movement of this fish[8]. They use the central pattern generator(CPG) network to generate periodic swimming motion of the bionic robotic fish, they also use the particle swarm optimization (PSO) algorithm to optimize the speed and the efficiency of the robotic fish.

Wang *et al.* designed a bionic mechanic crab. This crab has 8 legs including 6 3DOFs walking legs and two 3DOFs swimming paddles.[9] They proposed a novel subsea propulsion pattern named as crab bounding gait. Which has a better performance than the former mechanic crab.

Li *et al.* designed a bionic walking mechanism with superior performance and simple structure, they analyzed the walking gait of crab, then proposed a designed scheme of the crab walking mechanism. Through the experiment, it has a better performance than the wheel model car [10].

Qin *et al.* designed a novel bionic robotic crab, which has eight-legs and two pincers. It uses stepping motor to drive gear crank connecting rod mechanism to control the cross direction moving and turning of the bionic crab, the lifting and falling of pincers is also realized by controlling the stepping motor to drive gear and rack mechanism. Although The whole mechanism is very complex, the performance of walking is very well [11].

Xing *et al.* designed a hybrid locomotion system for an amphibious spherical robot. It has 12 servo motors and 4 spray motors. It can walk on the ground by using four legs. In the water, it can do underwater three-dimensional motion. They test the performance of this hybrid locomotive system, and the performance is relatively good [12-14].

Guo *et al.* designed a path planning system of a spherical Mobile Robot. This spherical robot also could walk on the ground and swim in the water. They designed a ground path planning system. In this path planning system, they use a hybrid algorithm include genetic algorithm (GA), the Ant colony algorithm (ACO), and they verified the performance of the hybrid algorithm is better than single GA or single ACO [15].

Guo *et al.* designed a wireless mobile environment monitoring system by using amphibious spherical robot. They used the temperature and humidity sensors and high definition cameras to collect the environmental information, the XBee module was used to communicate PC with the spherical robot. In collecting environmental data, they use an adaptive weighted fusion algorithm to deal with these data, it could also improve the data accuracy [16-18].

Hou *et al.* designed a novel thrust system for the amphibious sphere robot. They analyzed the hydrodynamic performance of this novel thruster, such as the thrust force in different rotating velocity and inlet velocity, used the Computational Fluid Dynamics (CFD) to simulate the hydrodynamic behavior. It is a very important basic research [19,20].

From the current design of bionic robots, we can see that the performance of bionic robots is better than the conventional robots (such as land wheel robots, underwater propeller propulsion robots). Liu researches a lot of animals' motions and refer to some bionic robots at home and abroad, then designed a mechanical structure for our bionic duck [21], as shown in the Fig. 1. We will introduce the structure of the bionic duck's leg in the second chapter, the mathematical model of bionic duck's leg in the third chapter, experiment and verification in fourth chapter, the last chapter is the conclusion and future work.

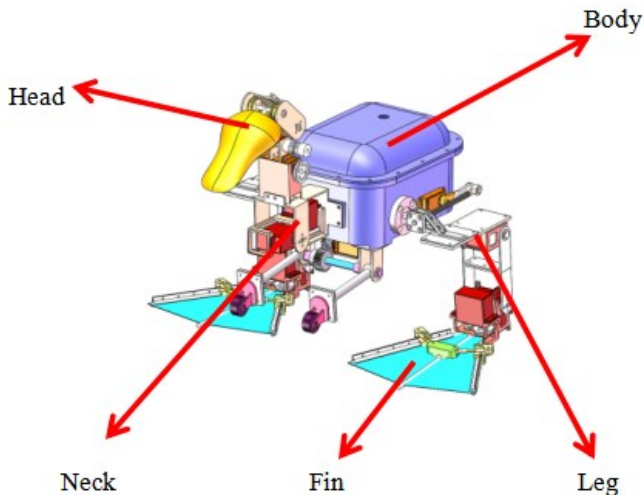


Fig. 1. The whole structure of the duck-like robot

II. THE INTRODUCTIONS OF TESTING DEVICE

A. The Mechanical Structure of Duck-like Robot's Leg

The mechanical structure of bionic duck leg consists of three parts, including thigh, calf, and swimming-fin, the thigh is driven by a crank structure, as is shown in the Fig. 2. The way which we drive the crank structure has two schemes. The first scheme is using an improved rotatable servo to drive. Because the leg is a bit heavy, we used a powerful rotatable servo motor. The torque of this servo is 22kg/cm. The second scheme is using a step motor to drive this crank. Because of our step motor has only 2kg/cm torque value, we add a reduction gear which has a speed ratio 10:1, then the output torque amplifies 10 times, and could reach 20kg/cm. To maintain the running accuracy in a long time, we use the latter scheme. When the step motor rotates, the metal rod is driven to swing up and down around the front shaft. The thigh will swing up and down which has an angle range from 45 degrees to (-45) degrees. The connection between thigh and calf, the connection between calf and swimming-fin, and closing and opening swimming-fin are all driven by servo motors, the swimming-fin has an angle range from 15 degrees to 45 degrees. The length of each connecting rod, the parameters of the servo motors and stepping motors used are shown in Tables I and II.

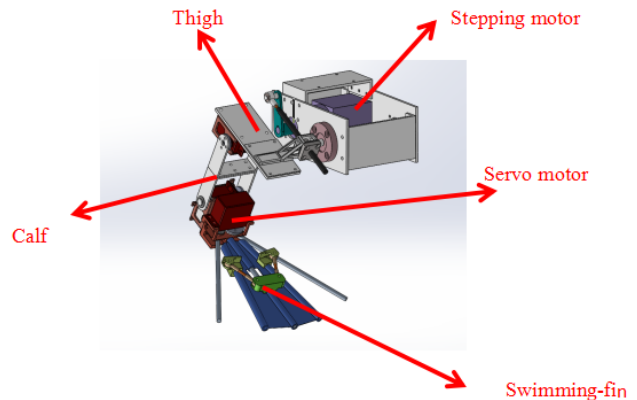


Fig. 2. The mechanical structure and corresponding driven devices

TABLE I
LENGTH OF LEG COMPONENTS

Name	Link1	Link2	Link3
Length(cm)	7.97	8.01	20.93

TABLE II
SPECIFICATION OF THE DRIVER COMPONENT

Servo motor	Thigh servo motors	6.6V: 23kg-cm, 0.12sec/60°
	Calf servo motors	6.6V: 23kg-cm, 0.12sec/60°
	Fin servo motors	6.6V: 23kg-cm, 0.12sec/60°
Stepping motor		24V, 1.8A

B. The Control Platform of the Duck-like Robot

The hardware platform of bionic duck is composed of two control circuit boards. The main control board is the Raspberry-Pi 3B. The main task of the main control board is doing object recognition, and reading the yaw angle from the gyroscope.

STM32F407VET6 was used on the auxiliary board, which is responsible for calculating the mathematical relationship between the end positions of the fin and the angles of servo motors, controlling servo and stepping motors and reading pressure data from the pressure sensors which goes through IIC communication protocol. The serial port communications protocol was used to communicate main control board with auxiliary control board. The main contents of communication include: the walking or swimming attitude control code from the main circuit board to auxiliary circuit board; the data of pressure sensor from the auxiliary board to main board. Besides, we adopted control-electric and power-electric isolation scheme, it means that the two circuit do not use the same ground. When the stepping motor is running, it usually requires huge current, so we designed a specific circuit board to drive the stepping motor. As shown in Fig. 3.

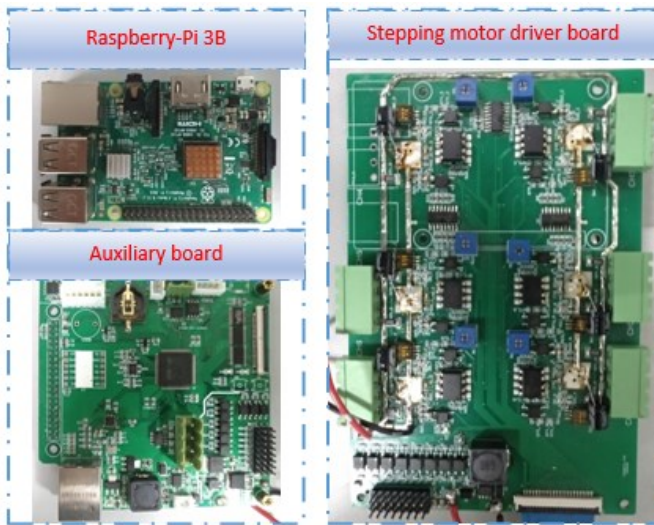


Fig. 3. Practical picture of the control circuit boards

On the software platform, the main control board uses the Ubuntu 16.04 mate version as its operational system, and carries the ROS kinetic version as its running platform, used to tackle multi-task synchronization. The auxiliary board uses the $\mu\text{COS-III}$, which is used for controlling the cooperation between servo motors and stepping motors, reading data from some sensors.

III. MATHEMATICAL MODEL OF BIONIC DUCK'S LEG

The motion of the leg can be considered as a cooperative motion of three bar linkage. Among them, the base coordinate system is set at the root connecting rod, and the sub-coordinate is set at each joint. The negative half axis of the x-axis of the sub-coordinate system is co-linear with the upper connecting rod. As is shown in the Fig. 4, the negative coordinate system 3 is co-linear with the coordinate system 2'. l_1, l_2, l_3 stand for the thigh, calf, fin of the duck-like robot respectively.

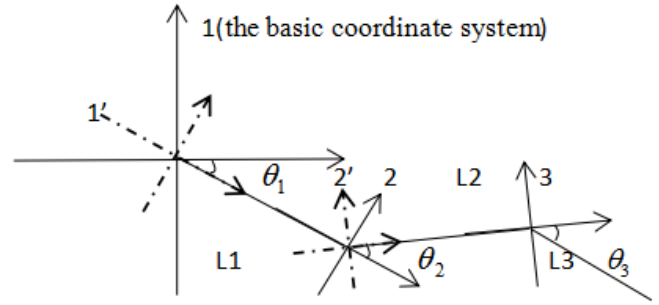


Fig. 4. Three-link coordinate system diagram

There is a strict mathematical relationship between the end positions of connecting rods and the angles of the connecting rods in each corresponding coordinate system. We will model and analyze this model and give strict mathematical relationship between the end position of connecting rod and the angles.

A. The Mathematical Relationship between Position and Angle

In coordinate system 3, the coordinates at the end of the connecting rod is:

$$\begin{bmatrix} x_3 \\ y_3 \end{bmatrix} = \begin{bmatrix} l_3 \cos \theta_3 \\ l_3 \sin \theta_3 \end{bmatrix} \quad (1)$$

Translate the coordinate system 3 to coordinate system 2', the coordinates in system 2' are as follows.

$$\begin{bmatrix} x_2' \\ y_2' \end{bmatrix} = \begin{bmatrix} l_3 \cos \theta_3 + l_2 \\ l_3 \sin \theta_3 + 0 \end{bmatrix} \quad (2)$$

Rotate system 2' to system 2 with $(-\theta_2)$, we need to multiply left by the rotation transformation matrix. In the coordinate system 2, the coordinates are:

$$\begin{bmatrix} x_2 \\ y_2 \end{bmatrix} = \begin{bmatrix} \cos(-\theta) & \sin(-\theta) \\ -\sin(-\theta) & \cos(-\theta) \end{bmatrix} \begin{bmatrix} l_3 \cos \theta_3 + l_2 \\ l_3 \sin \theta_3 \end{bmatrix} \quad (3)$$

Use the same method, the coordinates of the end of the connecting rod in the basic coordinate system can be obtained by translating to the coordinate system 1' and rotating to the system 1:

$$\begin{cases} x_1 = l_1 \cos \theta_1 + l_2 \cos(\theta_1 + \theta_2) + l_3 \cos(\theta_1 + \theta_2 + \theta_3) \\ y_1 = l_1 \sin \theta_1 + l_2 \sin(\theta_1 + \theta_2) + l_3 \sin(\theta_1 + \theta_2 + \theta_3) \end{cases} \quad (4)$$

B. The Calculation of Angle and Position

The coordinate value is calculated from the angle is a positive calculation process, while the angle calculate from the coordinate value is an inverse calculation process, In the actual process of controlling the duck's leg, the inverse solution is usually used to solve the angles. Since there are three unknowns in the equations, but the number of effect equations is two, it is necessary to take a special solution to one of the angles, and then solve the remaining two angles (term θ_1 as a special solution in actual calculation process). There are two method to calculate the two angles. The first is direct solution method, and the equations can also be regarded as non-linear equations and

use the Newton-Raphson method to solve them. Now describe the Newton-Raphson method.

For a function of one variable $y=f(x)$, use the Taylor Expansion, only the linear term is preserved, which is approximately equal to:

$$y=f(x) \approx f(x_0)+f'(x_0)(x-x_0) \quad (5)$$

Let $y=0$, After sorting out the formulas, we can get:

$$x=x_0-\frac{f(x_0)}{f'(x_0)} \quad (6)$$

The above expression is an expression that needs to be iterated over and over again in the program. When we calculate the value of x , and then put this value into x_0 , Stop iteration until the final calculated x value satisfies the accuracy or reaches the maximum iteration number.

Let θ_1 is a constant, computing θ_2 and θ_3 by expanding the above formula into the form of a matrix, we could obtain the following equations:

$$\begin{bmatrix} \theta_{21} \\ \theta_{31} \end{bmatrix} = \begin{bmatrix} \theta_{20} \\ \theta_{30} \end{bmatrix} - \begin{bmatrix} \frac{\partial f_2}{\partial \theta_2} & \frac{\partial f_2}{\partial \theta_3} \\ \frac{\partial f_3}{\partial \theta_2} & \frac{\partial f_3}{\partial \theta_3} \end{bmatrix}^{-1} \begin{bmatrix} f_2 \\ f_3 \end{bmatrix} \quad (7)$$

$\theta_2=\theta_{20}$
 $\theta_3=\theta_{30}$

θ_{21} and θ_{31} represent the $(k+1)$ times value of θ_2 and θ_3 respectively, θ_{20} and θ_{30} represent the k times value of θ_2 and θ_3 respectively, f_2 and f_3 are the following expressions:

$$\begin{cases} f_2=l_1 \cos \theta_1+l_2 \cos (\theta_1+\theta_2)+l_3 \cos (\theta_1+\theta_2+\theta_3)-x \\ f_3=l_1 \sin \theta_1+l_2 \sin (\theta_1+\theta_2)+l_3 \sin (\theta_1+\theta_2+\theta_3)-y \end{cases} \quad (8)$$

The iterative process is as follows:

1) Choose the initial value of θ_2 and θ_3 (θ_1 is a special value according to the swimming motion of the bionic duck leg).

2) Calculate the iteration equation.

3) Stop iteration according to termination condition, the termination condition is: the length of vector $[f_2, f_3]^T$ has satisfied the setting accuracy, or satisfied the maximum times of iterations. If the calculation results are not meet the termination condition, continue to do the first step.

IV. VERIFICATION EXPERIMENT

In this chapter, we tested two swimming modes. One is to imitate the swimming motion of ducks in water, the other is to imitate the swimming motion of fish swinging their tails in water. Comparing the two swimming modes, the peak value and the average value of the thrust was used to evaluate the performance of the maneuverability.

A. Swimming Mode I: Similar to duck

Swimming mode I is divided into four states. It takes 1/4 periods to switch from one state to another. It is accomplished by a stepping motor and three servo motors. The characteristic movements of the four states are shown in the four following figures (The initial position of swimming-fin is in state 1). The operation cycle was set 4.4s, 3.5s, 2.4s respectively.

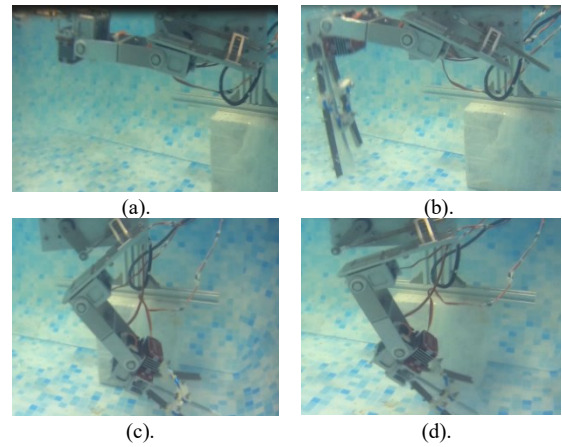


Fig. 5. Snapshots of the swimming mode I. (a) state1: kick leg. (b) state2: recovery and close the fin. (c) state 3: close the fin and get ready to kick. (d) state 4: open the fin and get ready to kick.

Different frequency will generate different forward thrust. The following table shows the forward thrust generated by the swimming-fin (note: the x-axis stands for time, the y-axis stands for forward thrust).

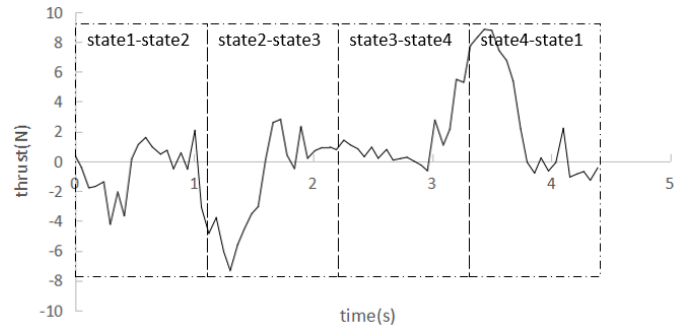


Fig. 6. Forward thrust of swimming mode I in one cycle of 4.4s

TABLE III
THE AVERAGE FORWARD THRUST IN ONE PERIOD OF 4.4 SECONDS

	State1-2	State2-3	State3-4	State4-1
Average thrust (N)	-0.6	-1.9	0.65	3.9

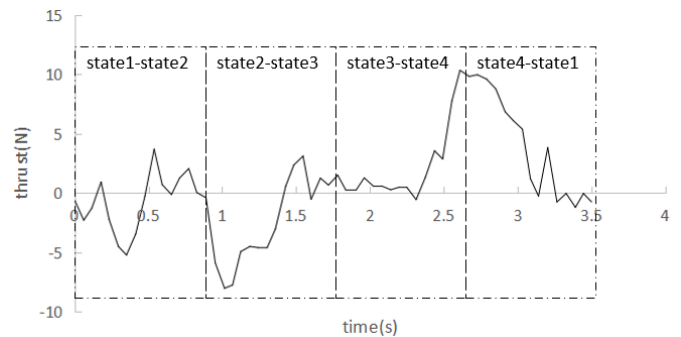


Fig. 7. Forward thrust of swimming mode I in one cycle of 3.5s

TABLE IV
THE AVERAGE FORWARD THRUST IN ONE PERIOD OF 3.5 SECONDS

	Stage1-2	Stage2-3	Stage3-4	Stage4-1
Average thrust(N)	-0.75	-2.4	1.7	4.2

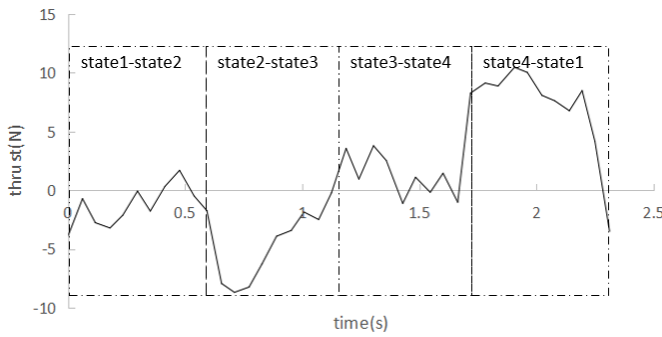


Fig.8. Forward thrust of swimming mode I in one cycle of 2.4s

TABLE V

THE AVERAGE FORWARD THRUST IN ONE PERIOD OF 2.4 SECONDS

	State1-2	State2-3	State3-4	State4-1
Average thrust(N)	-1.3	-4.48	1.9	7

Because the area of swimming-fin is a bit large, if the operation cycle is shortened, the huge torque will cause the stepping motor to lose synchronization. After tested, its minimum operating cycle is not less than 2.1 seconds.

As Shown in Fig. 6, Fig. 7, Fig. 8, and Table III, IV, V, we find that: in one cycle of 4.4 seconds, the peak thrust is 8.9N, the total average thrust is 0.51N; in one cycle of 3.5 seconds, the peak thrust is 10.34N, the total average thrust is 0.68N; in one cycle of 2.4 seconds, the peak thrust is 10.45N, the total average thrust is 0.78N. With the increase of operational frequency, its average forward thrust increases gradually. Especially in the process from state4 to state1, the forward thrust increases significantly, reaching 7N in a period of 2.4 seconds.

B. Swimming Mode II: Similar to fish, two-joint cruise

Swimming mode II is divided into two states. The stepping motor maintains a constant position, the swimming-fin opens all the time, and the remaining two servo motors work together to complete the whole actions. The characteristic movements of the two states are shown in the following figures (The initial position of swimming-fin is in state 1). The operation cycle of experiment was set 4.4s, 3.1s, 2.3s respectively.

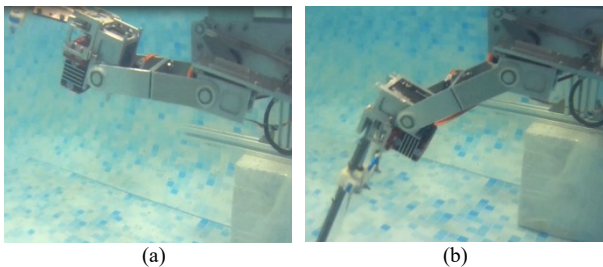


Fig. 9. Snapshots of the swimming mode II. (a) state 1: downward swing; (b) state 2: upward swing.

The up-and-down swing of the legs will generate the force to push the duck-like robot to swim forward. The following figures and tables show the forward propulsion force produced by swimming-fin in different operation cycles (note: the x-axis stands for time, the y-axis stands for forward thrust).

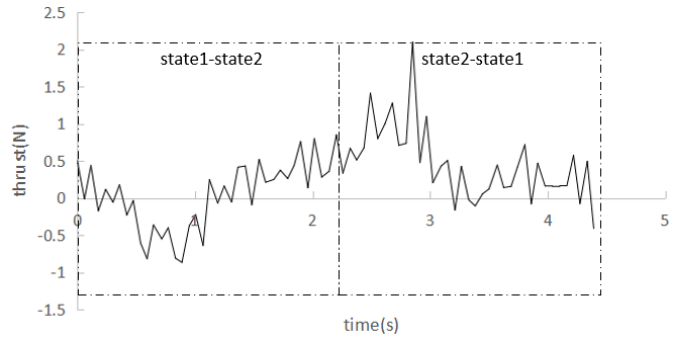


Fig. 10. Forward thrust of swimming mode II in one cycle of 4.4s

TABLE VI

THE AVERAGE FORWARD THRUST IN ONE PERIOD OF 4.4 SECONDS

	State2-1	State1-2
Average thrust(N)	0.085	0.44

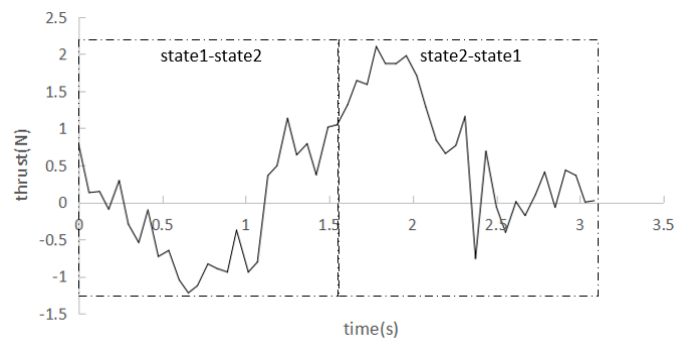


Fig.11. Forward thrust of swimming mode II in one cycle of 3.1s

TABLE VII

THE AVERAGE FORWARD THRUST IN ONE PERIOD OF 3.1 SECONDS

	State2-1	State1-2
Average thrust(N)	0.17	0.76

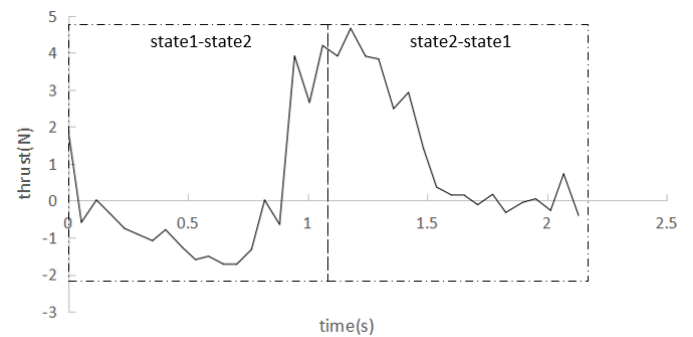


Fig.12. Forward thrust of swimming mode II in one cycle of 2.3s

TABLE VIII

THE AVERAGE FORWARD THRUST IN ONE PERIOD OF 2.3 SECONDS

	State2-1	State1-2
Average thrust(N)	0.32	1.57

If the operation cycle continues to be reduced, the up and down swing speed will continue to increase, and the servo motor will bear tremendous torque. If the operation cycle is reduced to less than one cycle of 2.2 seconds, the motion of the servo motors will be very uncoordinated.

As shown in Fig.10, Fig. 11, Fig. 12, and table VI, VII, VIII, we find that: in one cycle of 4.4 seconds, the peak thrust is 2.09N, the total average thrust is 0.26N; in one cycle of 3.1 seconds, the peak thrust is 2.1N, the total average thrust is 0.465N; in one cycle of 2.3 seconds, the peak thrust is 3.9N, the total average thrust is 0.945N. With the shortening of operation cycle, the average forward thrust increases gradually, in one cycle of 2.3 seconds, the average forward thrust is ideal. However, its peak forward thrust is not very large, its peak thrust is still less than 4N.

V. CONCLUSION AND FUTURE WORK

Both swimming modes have their own advantages and disadvantages. From the first swimming mode, we can see that from state 4 to state 1, the average thrust produced by the bionic duck's swimming fin is ideal, and even reaches 7N in the 2.4 seconds cycle of motion. However, the overall average thrust is not optimistic, the maximum is only 0.78N. From the second swimming mode, we can see that the average thrust of this mode of operation is very small in relatively slow motion, or almost no thrust, but when the speed of operation is increased to 2.3 seconds of a cycle, the forward thrust generated is very considerable, almost reaching 1N. To summary, we can adopt such a swimming control strategy: in the initial stage, using state 4 to state 1 of the first swimming mode to raise the swimming speed of bionic ducks in a short period of time, and then switching to swimming mode II of the 2.3 seconds of a cycle quickly, providing a relatively stable, large forward thrust to help bionic ducks run for a long time. We also have another strategy: during the experiment, We found that the average forward thrust in swimming mode I is relatively small, it was caused by the reverse force in the process of retrieving the swimming-fin, because the area of the swimming-fin was relatively large. So we can appropriately reduce the area of swimming-fin. When the ankle reaches the highest point, the swimming-fin can be retracted away from the above of water surface, which can increase the average forward thrust of swimming mode I.

In future work, we will make some improvements on the mechanical structure of bionic duck's swimming-fin, we will test the whole duck-like robot, in order to test the swimming performance of duck-like robot under the above two control strategies.

ACKNOWLEDGEMENT

This research is partly supported by the National High Tech. Research and Development Program of China (No.2015AA043202), and National Natural Science Foundation of China (61773064, 61503028), Graduate Technological Innovation Project of Beijing Institute of Technology (2018CX10022) and National Key Research and Development Program of China (No. 2017YFB1304401).

REFERENCES

[1] Y. Tan, D. Wang, H. Xu, et al. "Rapid Recovery Hydrogel Actuators in Air with Bionic Large-Ranged Gradient Structure". *ACS Applied Materials & Interfaces* 2018, vol. 10, no. 46, pp. 40125-40131.

[2] X. Wang, W. Song, M. You, et al. "Bionic Single-Electrode Electronic Skin Unit Based on Piezoelectric Nanogenerator". *ACS Nano*, 2018, vol.2, no.8, pp. 8588-8596.

[3] J. Zhong, M. Luo, X. Liu, et al. "Frog-Inspire Jumping Robot Actuated by Pneumatic muscle actuators". *Advances In Mechanical Engineering*, vol. 10, no. 6, pp. 2-5, 2018.

[4] F. Zhang, L. Zheng, W. Wang, et al. "Development of Agriculture Bionic Mechanisms: Investigation of the Effect of Joint Angle and Pressure on the Stability of Goats Moving on Sloping Lands". *International Journal of Agriculture and Biological Engineering*, vol. 11, no. 3, pp. 35-41, 2018.

[5] Y. Wang, J. Zhu, X. Wang, et al. "Hydrodynamics Study and Simulation of A Bionic Fish Tail Driving System Based on Linear Hypocycloid ". *International Journal of Advanced Robotic Systems*, vol. 15, no. 2, 2018.

[6] G. Wang, Y. Song, W. Tang, et al. "A Numerical Simulation Analysis on Bionic Robotic Fish Based on Computational Fluid Dynamics (CFD) Method". *Journal of Nanoelectronics and Optoelectronics*, vol. 14, no. 3, pp. 400-407, 2019.

[7] A. Wicaksono, S. Hidayat, B. Retnoaji, et al. "A Mechanical Piston Action May Assist Pelvic-Pectoral Fin Antagonism in Tree-Climbing Fish". *Journal of The Marine Biological Association of The United Kingdom*, vol.8, no.8, pp. 2121-2131, 2018.

[8] M. Wang, F. Dong, X. Li, et al. "Control and Optimization of A Bionic Robotic Fish Through A Combination of CPG and PSO". *Neurocomputing*, vol. 337, no. 1, pp. 144-152, 2019.

[9] G. Wang, X. Chen, S. Yang, P. Jia, et al. "Subsea Crab Bounding Gait of Leg-Paddle Hybrid Driven Shoal Crablike Robot", *Mechatronics*, vol. 48, no. 2, pp. 1-11, 2017.

[10] J. Li, G. Zhang, Y. Wang, et al. "Bionic Crab Walking Mechanism And Its Kinematic Characteristic Analysis", *Transactions of the Chinese's Society of Agricultural Engineering*, vol. 32, no. 14, pp. 47-54, 2016.

[11] H. Qin , Z. Zheng, Y. Liu, et al. "Design of Structure Bionic Crab-Like Robot Based On Gear Transmission", *Journal of Mechanism Transmission*, vol. 39, no. 7, pp. 79-82, 2019.

[12] H. Xing, S. Guo, L. Shi, et al. "Hybrid Locomotion Evaluation for a Novel Amphibious Spherical Robot", *Applied Science*, vol. 8, no. 156, pp. 1-4, 2018.

[13] H. Xing, L. Shi, K. Tang, S. Guo, X. Hou, Y. Liu, H. Liu, Y. Hu. "Robust RGB-D Camera and IMU Fusion-based Cooperative and Relative Close-range Localization for Multiple Turtle-inspired Amphibious Spherical Robots", *Journal of Bionic Engineering*, vol.16, no.3, pp.442-454, 2019.

[14] H. Xing, S. Guo, L. Shi, S. Pan, Y. He, K. Tang, S. Su, Z. Chen. "Kalman filter-based navigation system for the amphibious spherical robot", in *Proceedings of the IEEE International Conference on Mechatronics and Automation*, Takamatsu, Japan, 2017, pp. 638-643.

[15] J. Guo, C. Li, et al. "Application of the Hybrid Algorithm in Path Planning of the Spherical Mobile Robot", in *Proceeding of the IEEE International Conference on Mechatronics and Automation*, Changchun, China, 2018, pp.323-328.

[16] S. Guo, X. Yang, J. Guo, et al. "Design of Wireless Mobile Environment Monitoring System Based on Spherical Amphibious Robot", in *Proceedings of the IEEE International Conference on Mechatronics and Automation*, Changchun, China, 2018, pp. 960-965.

[17] L. Zheng, S. Guo, S. Gu, "The communication and stability evaluation of amphibious spherical robots", *Microsystem Technologies*, vol. 24, pp. 1-12, 2018.

[18] S. Pan, L. Shi, S. Guo, "A Kinect-based real-time compressive tracking prototype system for amphibious spherical robots", *Sensors*, vol. 15, pp. 8232-8252, 2015.

[19] X. Hou, S. Guo, L. Shi, et al. "Hydrodynamic Analysis of a Novel Thruster for Amphibious Spherical Robot", in *Proceeding of the IEEE International Conference on Mechatronics and Automation* Changchun, China, 2018, pp. 1603-1608.

[20] X. Hou, S. Guo, L. Shi, H. Xing, Y. Liu, H. Liu, Y. Hu, D. Xia, Z. Li, "Hydrodynamic Analysis-Based Modelling and Experimental Verification of a New Water-Jet Thruster for an Amphibious Spherical Robot", *Sensors*, vol. 19, 259, 2019.

[21] H. Liu, L. Shi, S. Guo. "Platform Design for a Natatores-like Amphibious Robot", in *Proceeding of IEEE International Conference on Mechatronics and Automation*, Changchun, China, 2018, pp. 1627-1632.